

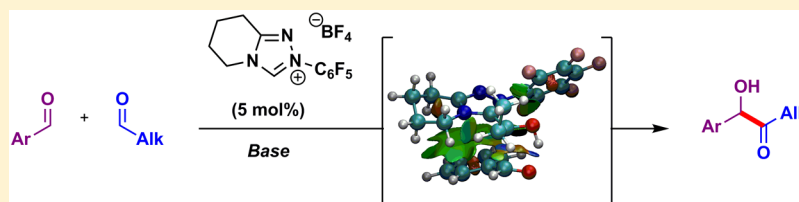
Origin of Chemoselectivity in N-Heterocyclic Carbene Catalyzed Cross-Benzoin Reactions: DFT and Experimental Insights

Steven M. Langdon,[†] Claude Y. Legault,^{*,‡} and Michel Gravel^{*,†}

[†]Department of Chemistry, University of Saskatchewan, 110 Science Place, Saskatoon, Saskatchewan S7N 5C9, Canada

[‡]Département de Chimie, Université de Sherbrooke, 2500 Boulevard Université, Sherbrooke, Quebec J1K 2R1, Canada

S Supporting Information



ABSTRACT: An exploration into the origin of chemoselectivity in the NHC-catalyzed cross-benzoin reaction reveals several key factors governing the preferred pathway. In the first computational study to explore the cross-benzoin reaction, a piperidinone-derived triazolium catalyst produces kinetically controlled chemoselectivity. This is supported by ¹H NMR studies as well as a series of crossover experiments. Major contributors include the rapid and preferential formation of an NHC adduct with alkyl aldehydes, a rate-limiting carbon–carbon bond formation step benefiting from a stabilizing π -stacking/ π -cation interaction, and steric penalties paid by competing pathways. The energy profile for the analogous pyrrolidinone-derived catalyst was found to be remarkably similar, despite experimental data showing that it is less chemoselective. The chemoselectivity could not be improved through kinetic control; however, equilibrating conditions show substantial preference for the same cross-benzoin product kinetically favored by the piperidinone-derived catalyst.

INTRODUCTION

Originally reported in 1832 by Wöhler and Liebig,¹ the benzoin reaction is the coupling of two aldehydes to form an acyloin. The groups of Ukai² and Breslow³ described how thiazolium salts could also catalyze this reaction in the presence of base. Much later, other N-heterocyclic carbene (NHC) catalysts were shown to effect the same transformation.⁴ Breslow proposed the currently accepted mechanism, based on analogy to Lapworth's mechanism for the cyanide-catalyzed benzoin reaction (Scheme 1).^{3,5}

First, deprotonation of the salt (I) generates the active carbene catalyst (II). This nucleophilic species then attacks 1 equiv of aldehyde, generating an intermediate (III) that is rapidly protonated to form a carbene–aldehyde adduct (IV). Deprotonation of this adduct generates a resonance-stabilized zwitterion now referred to as the Breslow intermediate (V). This species is crucial to the reaction, as it induces a reversal of polarity (*umpolung*), making the previously electrophilic carbonyl carbon nucleophilic.⁶ The Breslow intermediate then attacks another 1 equiv of aldehyde and undergoes a proton transfer that is either concerted or stepwise ([V–VI]). Collapse of this species (VI) releases the benzoin (acyloin) product and reintroduces the catalyst into the cycle.

This reaction lends itself quite well to homocoupling reactions of aldehydes, and the majority of early work focused on these reactions.^{4b,7} Triazolium catalysts in particular are known for their high efficiencies and enantioselectivities in homocoupling benzoin reactions. However, benzoin reactions between two different aldehydes are substantially more challenging than

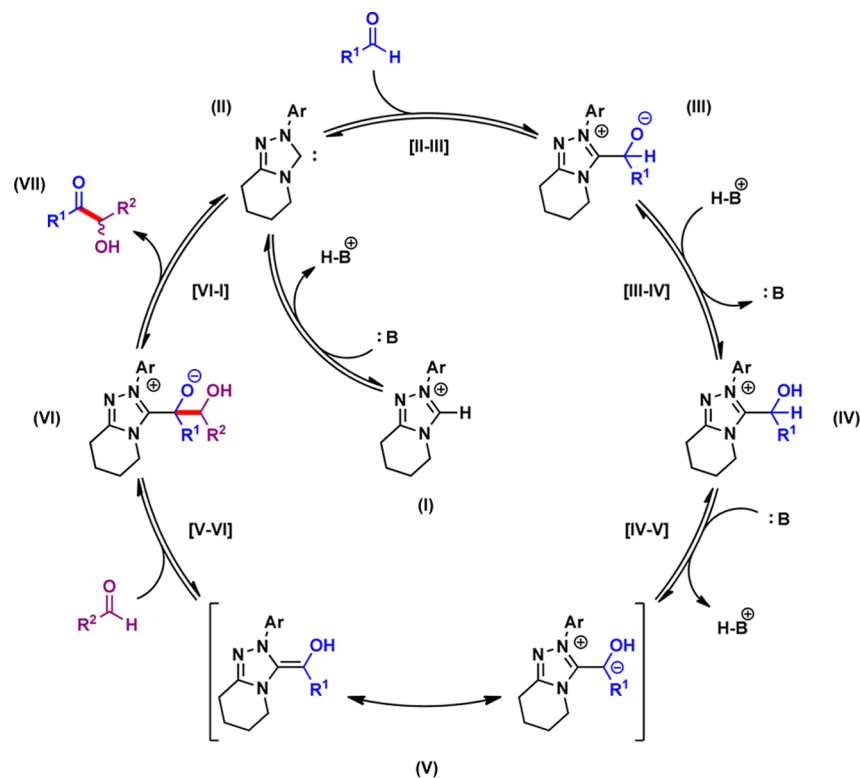
homocouplings.^{4j} The problem can most easily be attributed to one of reactivity; if one aldehyde is preferred for formation of the Breslow intermediate, such as by being more accessible or having greater electrophilicity, then it should also be preferred for the carbon–carbon bond formation step.⁸ If steric and electrophilic factors are similar between the two aldehydes, then there is no impetus for chemoselectivity and a statistic and/or thermodynamic mix of the four possible products is obtained. The reversibility of the majority of benzoin reactions exacerbates problems with achieving kinetic selectivity, although it can be exploited in situations where the desired product is also the thermodynamic product. Chemoselectivity achieved in this way may not have general applicability, particularly if enantioselectivity is also a concern. On the basis of these considerations, kinetically controlled chemoselectivity must rely on substrate, condition, and/or catalyst control.

Several approaches to chemoselective cross-benzoin reactions exist. The simplest of these is to tether two potential partners within a molecule; several chemoselective intramolecular cross-benzoin reactions have been reported, relying on entropy to overcome differences in reactivity between the two moieties.⁹ Intermolecular cross-benzoin reactions can be made chemoselective by including a large excess of one aldehyde.¹⁰ In these cases the cross-benzoin product usually corresponds to that from the Breslow intermediate being formed with the aldehyde in

Received: February 9, 2015

Published: March 3, 2015

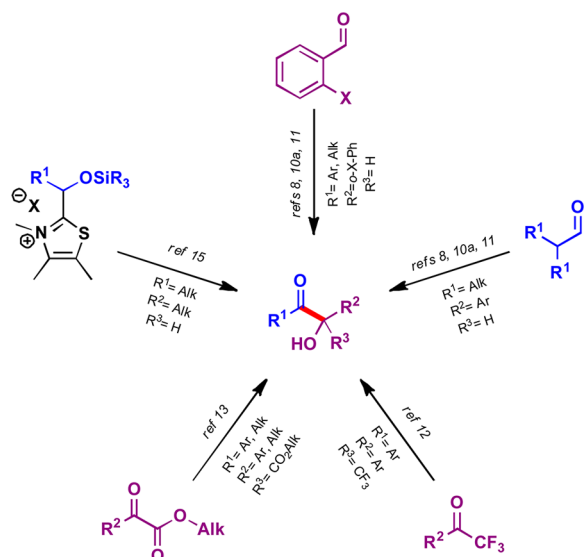
Scheme 1. Mechanism of the Benzoin Reaction



excess, and a large amount of the homocoupled product is also obtained. While potentially versatile, this approach may be limited in synthetic usefulness.

A handful of methods are available for stoichiometric and near-stoichiometric situations, each relying on substrate control (Scheme 2). The use of ortho-substituted aromatic aldehydes

Scheme 2. Approaches to Chemoselective Intermolecular Cross-Benzoin Reactions

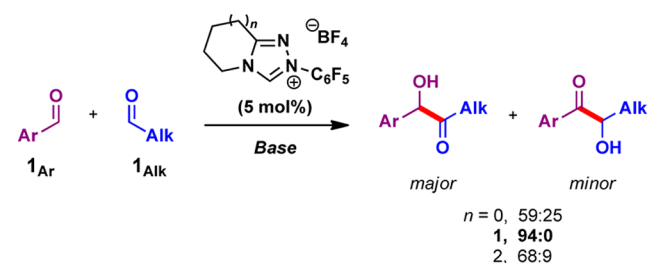


and/or α -branched aliphatic aldehydes results in moderate to high chemoselectivity and was first demonstrated by Stetter and Dämbkes in the 1970s.^{8,10a,11} Fluorinated acetophenone derivatives,¹² α -keto esters,¹³ and ketones^{9a-g,14} also produce

chemoselective reactions, as they are unable to form the Breslow intermediate but may be attacked in the carbon–carbon bond forming step ([V–VI]). These approaches have the advantage of using easily accessible substrates but are conversely restricted in potential scope as a result. Scheidt's group has developed a noncatalytic method using *O*-silyl thiazolium carbinols, theoretically allowing access to any desired cross-benzoin product.¹⁵ This route is unique in having the costs and benefits opposite to those previously described; the substrates are not easily accessible, but the scope is potentially broad. Related work with ThDP-dependent benzaldehyde lyase has also generated cross-benzoin products chemoselectively, though on relatively small scales.¹⁶

We recently disclosed the first general approach to chemoselective cross-benzoin reactions which relied on catalyst rather than substrate control (Scheme 3).¹⁷ A change from the

Scheme 3. Catalyst-Controlled Chemoselective Intermolecular Cross-Benzoin Reaction



traditional pyrrolidinone-based salt to a piperidinone-based triazolium catalyst resulted in a dramatic improvement in chemoselectivity. The reasons for this improvement were not immediately apparent. Preliminary experiments confirmed that

the selectivity was kinetically derived. As well, the rate-limiting (viz. chemoselectivity-determining) step was found to be at least second order.

Computational studies provide an excellent method for probing mechanistic challenges. Previous density functional theory (DFT) investigations into the benzoin reaction have focused primarily on non-NHC catalysts.¹⁸ Even in studies of NHC catalyzed reactions the focus has primarily been on the Stetter reaction.¹⁹ Within those studies which focus on the benzoin reaction, attention has been limited to homo-benzoin reactions. In 2004 Dudding and Houk published the first major study in this area, focusing exclusively on the carbon–carbon bond formation step ([V-VI]).²⁰ The work used a variation of ONIOM (*n*-layered integrated molecular orbital method) with a combination of B3LYP/6-31G(d) and AM1 levels of theory to determine relative energies of diastereomeric transition states for chiral triazolium- and thiazolium-catalyzed reactions. Fundamentally, this study cemented the presence of a concerted proton transfer during this phase of the reaction. This necessitates a five-membered ring and dramatically limits the number of possible conformers to be considered in this step.

More recently an *N*-alkyl triazolium catalyst was modeled for the homocoupling of benzaldehyde.²¹ The study determined that the rate-limiting step was most likely formation of the Breslow intermediate ($\Delta G = 28.8\text{--}30.9$ kcal/mol) using the B3LYP functional with the 6-31+G(d) and 6-311+G(2d,p) basis sets. However, the possibility of a stepwise proton transfer mediated by the base/conjugate acid was not explored. The attacks on aldehydes ([II-III] and [V-VI]) were found to be the second highest barriers at 24.1 and 27.0 kcal/mol, respectively.

Finally, the Nyulászai group recently reported a study comparing benzoin reactions as catalyzed by thiazolium and triazolium catalysts.²² While Gibbs free energies were not determined, self-consistent field (SCF) energies at the B3LYP/6-311+G** level were shown. The authors note that NHC–aldehyde adducts are significantly lower in energy than the Breslow intermediate, though only the energy of the Berkessel adduct (the keto tautomer of the Breslow intermediate)²³ was calculated. Again the rate-limiting step was found to be the proton transfer leading to the Breslow intermediate, though the authors suggest that this could change in a stepwise base-mediated scenario. Although not the focus of the report, the study also found that the barrier for the carbon–carbon bond formation step ([V-VI]) with acetaldehyde and its triazolium-derived Breslow intermediate is 3.5 kcal/mol higher in energy than the ejection ([VI-I]) step. This is reversed in the same steps with the thiazolium-derived Breslow intermediate; the ejection step is 2.9 kcal/mol higher in energy than the carbon–carbon bond forming step.

As previously mentioned, each of these studies has been limited to discussions of homo-benzoin reactions. This has been reasonable, as it dramatically lowers the number of possible conformers and transition states needed to examine the reaction as a whole. However, this also means that subtle differences between closely related species (i.e., isomers of VI and its associated transition states) have not yet been explored. Probing such differences is crucial in considering the cross-benzoin reaction (Scheme 3), as many structures in competing paths are isomeric.

Computational results can provide a great deal of insight into reaction mechanisms, but they are best accompanied by experimental results to corroborate and enhance the picture they create. It was previously demonstrated that the reaction is at

least second order. In the present work, a more rigorous determination confirms the possible rate-limiting steps on the basis of the species involved and rules out more exotic possibilities containing greater than two aldehydes. Crossover experiments establish which paths are reversible and irreversible and support claims of kinetic selectivity. Finally, monitoring reactions by ¹H NMR allows final verification of kinetic selectivity and grants some insight into which species are formed during the course of the reaction. Combining these results paints a vivid picture of the potential uses and limitations of the current methodology, granting future users a dossier to consult when planning uses of this methodology.

■ COMPUTATIONAL METHODS

All calculations were performed with the Gaussian 09 software package.²⁴ On comparison of closely related structures, small changes from noncovalent interactions (i.e., London dispersion forces, π interactions) may have a pronounced effect on the calculated energy. As it accounts for these interactions, the M06-2X functional seems appropriate for this investigation;²⁵ the M06-2X exchange-correlation functional with the polarized diffuse split-valence 6-31+G(d,p) basis set was used in all cases. Subsequent single-point energies were determined using the corresponding triple- ζ 6-311+G(d,p) basis set. Solvent effects were added using the integral equation formalism model (IEFPCM)²⁶ with radii and nonelectrostatic terms for Truhlar and co-workers' SMD solvation model (CH₂Cl₂).²⁷

For each species a broad conformational search was performed typically using the MMFF94 force field. Some additional conformers were generated by hand as needed. The lowest energy structures (typically 20–30) were carried forward for full optimization. The conformer with the lowest energy had its vibrational frequencies computed using the same level of theory to confirm that it was an energy minimum and to evaluate its zero-point vibrational energy (ZPVE) and thermal corrections at 298.15 K.

Transition states were found using a similar conformer search, but with a single constrained interatomic distance. The lowest energy conformers found with this process were optimized without the constraint and confirmed to be first-order saddle points by harmonic vibrational frequency analysis. The imaginary frequency was inspected in each to ensure it represented the desired reaction coordinate, and the transition state with the lowest energy was chosen to represent the transformation. For key transition states the intrinsic reaction coordinate (IRC) was followed to ensure it connects the reactants and products.

Noncovalent interactions (NCIs) were plotted using NCIPLOT version 1.0 with the coordinates from the optimized structure/transition state.²⁸ Three-dimensional representations were generated using CYLview.²⁹

Energy differences between half-chair conformers on the catalyst backbone were typically found to be within the error of the calculation (usually ~ 0.5 kcal/mol) and are excluded from discussion. Counterion (BF₄[−]) placement was found to have a substantial effect on the energy of all charged species. In these cases the counterion was placed in several likely locations and these complexes were then optimized as above. Trimethylamine was modeled as a Hünig's base equivalent.

The reaction pathways reported below represent the minimum energy pathway (MEP), or a representative member thereof, for the transformation. Each of the four possible pathways was explored to the same extent for the reaction between benzaldehyde and propanal. For a summary of all energies for all possible pathways, see the Supporting Information.

■ RESULTS AND DISCUSSION

Alkyl–Alkyl Dimerization. The most straightforward case to consider is the homo-benzoin reaction of alkyl aldehydes. Propionaldehyde (**1_p**) was chosen for its simplicity and resemblance to the prototypical example (hydrocinnamaldehyde).

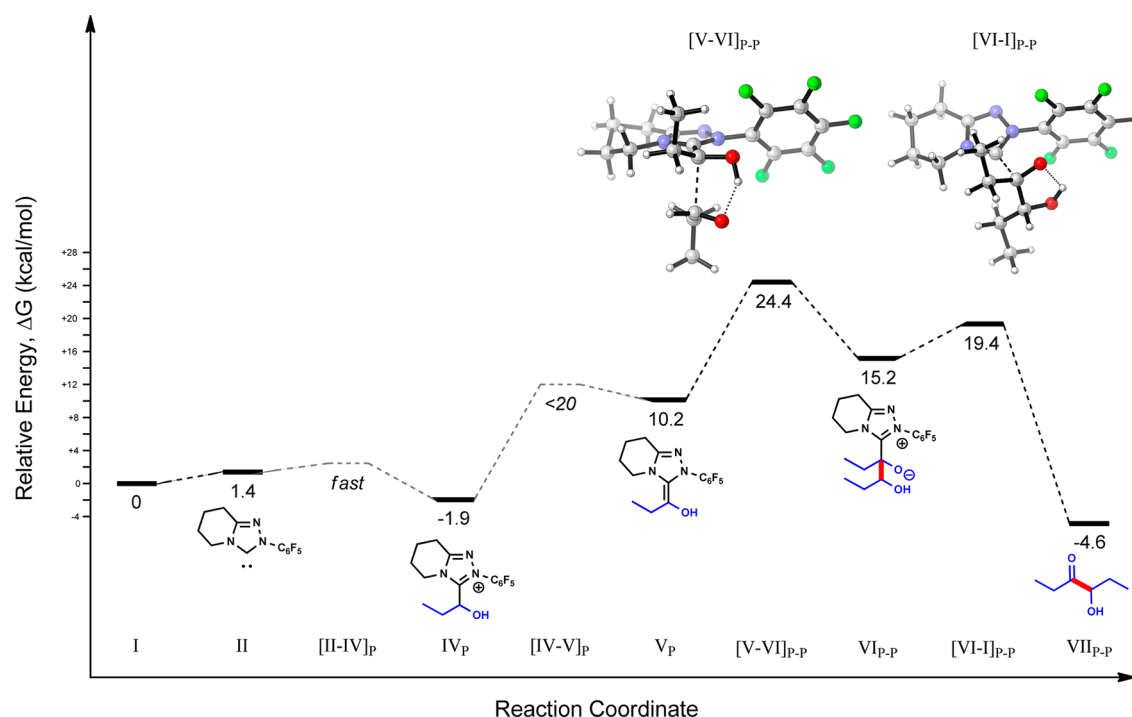


Figure 1. Alkyl-alkyl homo-benzoin reaction coordinate.

Scheme 4. Alkyl Adduct Formation

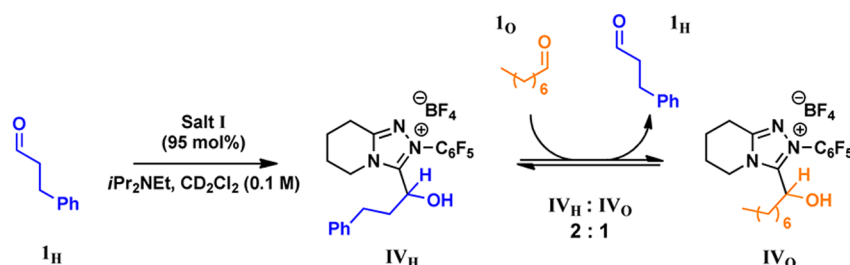


Figure 1 details the energy profile for this process and includes inset depictions of the optimized geometries for the carbon-carbon bond forming and ejection steps ($[V-VI]_{p-p}$ and $[VI-I]_{p-p}$).

Generation of the free carbene (**II**) is barrierless, and the carbene itself is slightly higher in energy (1.4 kcal/mol).

Attack on **I_p** ($[II-IV]_p$) generates the stable adduct **IV_p** at -1.9 kcal/mol. Several attempts were made to model this transition state ($[II-III]_{p-p}$) given previous group's findings.^{21,22} When none could be found, an experiment was performed with high catalytic loading and monitored by 1H NMR (Scheme 4). Formation of **IV_H** was found to be extremely facile, occurring within the first minute of the reaction at a near-quantitative level.³⁰ Addition of a second aldehyde, octanal, resulted in exchange and equilibration to a mixture of **IV_H** and **IV_O** rather than formation of any benzoin product(s). Consequently, it was concluded that the barrier for this step is relatively low, and that subsequent protonation ($[III-IV]$) is concomitant or lower still. The ensuing deprotonation leads to the formation of the Breslow intermediate (**V_p**). Though this transition state could also not be located, previous studies and our own finding that the reaction is second-order in aldehyde suggest that it is not rate-limiting.^{17,31} Both the *E* and *Z* isomers of **V_p** were modeled and found to have, within error, the same

energy (9.9 and 10.2 kcal/mol respectively). Ensuing steps are reported using the *Z* isomer to enhance comparability to the preferred path of the cross-benzoin reaction (*vide infra*).

There are two possible diastereomeric transition states for the carbon-carbon bond forming step ($[V-VI]_{p-p}$) resulting from attacks on the *re* and *si* faces of propionaldehyde. For this homo-benzoin reaction these attacks have comparable barriers (24.9 and 24.4 kcal/mol respectively) as there are few factors governing the incoming aldehyde's orientation save the five-membered hydrogen-bonding ring. The proton transfer is concomitant though asynchronous, appearing as a "hidden" intermediate in the IRC. The resulting intermediate (**VI_{p-p}**) is more energetic than the Breslow intermediate at 15.2 kcal/mol, and collapses comparatively quickly through ejection of the homo-alkyl benzoin product with a barrier of 19.4 kcal/mol. The resulting species are substantially more stable than starting materials at -4.6 kcal/mol.

A pair of crossover experiments subjected the homo-benzoin product of hydrocinnamaldehyde (**VII_{H-H}**) to reaction conditions to determine its reversibility (Scheme 5). The presence of neither aryl nor alkyl aldehydes led to the formation of any cross-benzoin product(s); the formation of **VII_{H-H}** and by extension most homo-benzoin products of alkyl aldehydes, is effectively irreversible under these conditions. Based on the rate-limiting

Scheme 5. Homo-Alkyl Crossover Experiments

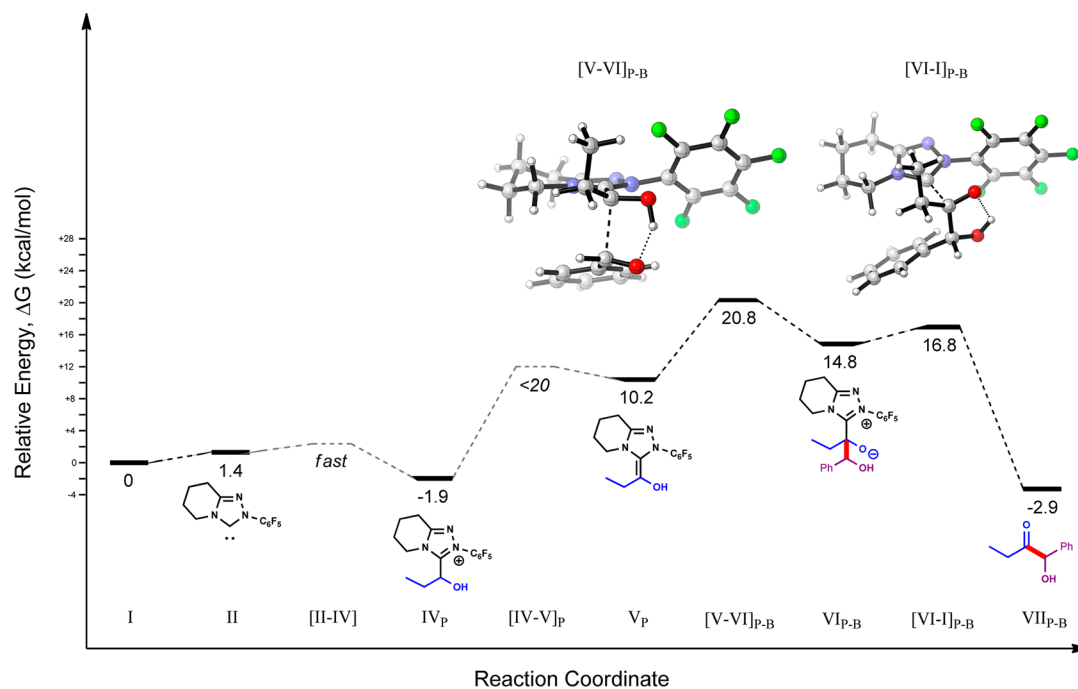
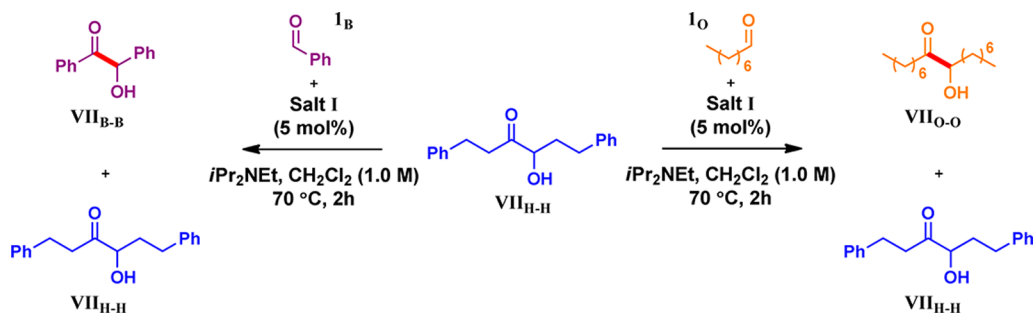


Figure 2. Alkyl-aryl cross-benzoin reaction coordinate.

step in the forward reaction being carbon-carbon bond formation, it is likely this is the irreversible step, though an irreversible catalyst ejection cannot be ruled out.

Alkyl-Aryl Cross-Benzoin. The major product in this reaction is the cross-benzoin product resulting from an alkyl aldehyde's Breslow intermediate attacking an aromatic aldehyde. Previous results have shown that this reaction is first order with respect to hydrocinnamaldehyde.¹⁷ These results were less conclusive with respect to benzaldehyde, suggesting that it may be greater than first order with respect to it. In order to rule out more exotic possibilities for the rate-limiting step, a rigorous examination of the reaction under a variety of substrate concentrations was performed (See Supporting Information). These confirmed that the reaction is not greater than first order with respect to benzaldehyde, allowing the examination to focus on the traditional pathway. The energy profile for this transformation is depicted in Figure 2. The reaction begins in the same fashion as above until the carbon-carbon bond formation step ($[V-VI]_{P-B}$). Here there is a clear preference for the attack on the *si* face of benzaldehyde from the *Z* Breslow intermediate; at 20.8 kcal/mol, this transition state is more than 2 kcal/mol lower than any of the three other possible diastereomeric transition states.

A comparison of these transition states reveals a likely source for this selectivity: a competition between the stabilizing effect of the approaching phenyl ring being beneath the triazole/developing cation and steric repulsion between substituents on the incoming and *N*-bound aryl groups. In the preferred transition state the best overlap of the benzaldehyde and triazole's π systems is achieved without significant steric interactions. A plot of NCIs was examined (Figure 3) and found to display a relatively strong π -stacking/ π -cation interaction, supporting this hypothesis. This stabilizing force is

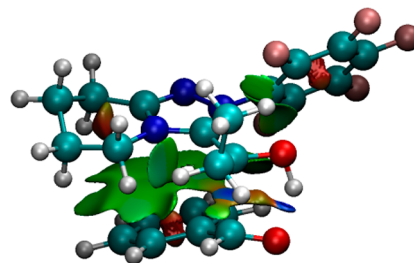


Figure 3. NCI plot of the carbon-carbon bond formation step of the alkyl-aryl cross-benzoin.

Scheme 6. Alkyl–Aryl Crossover Experiment

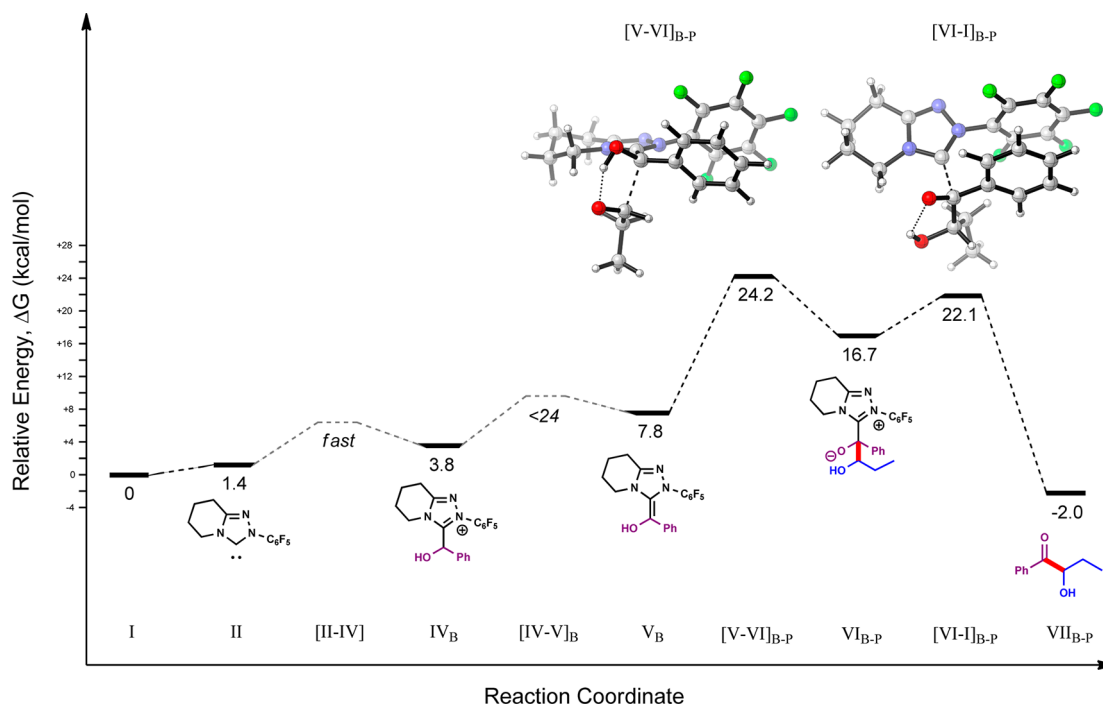
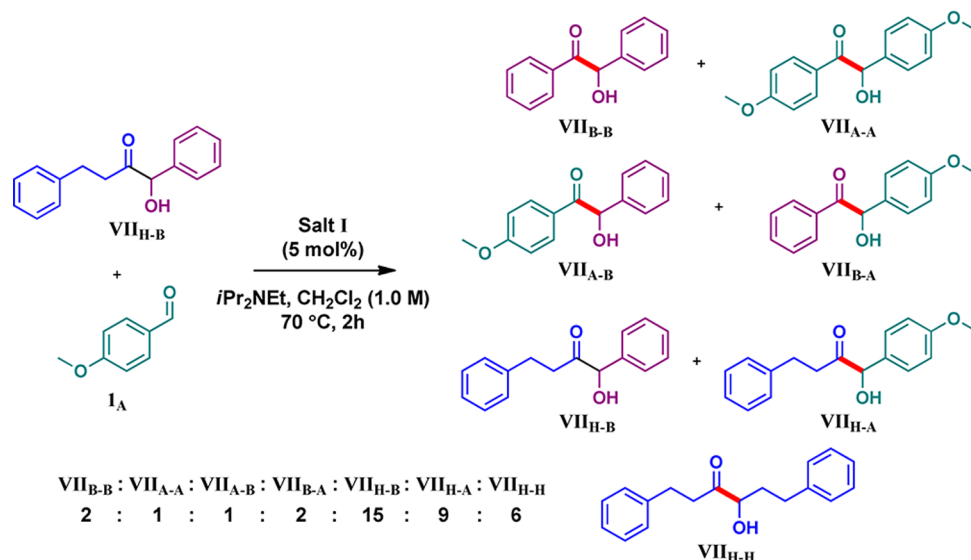


Figure 4. Aryl–alkyl cross-benzoin reaction coordinate.

also present in the resulting intermediate ($\text{VI}_{\text{P-B}}$) at 14.8 kcal/mol and during the transition state for the ejection of the product ($[\text{VI-I}]_{\text{P-B}}$) at 16.8 kcal/mol, resulting in both being significantly lower in energy than their diastereomeric counterparts. The product here is also more stable than starting materials at -2.9 kcal/mol, slightly higher than for the homo-alkyl product.

Again a crossover experiment was performed on the cross-benzoin product of hydrocinnamaldehyde and benzaldehyde (Scheme 6). Under reaction conditions, and in the presence of *p*-anisaldehyde, formation of the cross-benzoin product is found to be completely reversible; the formation of $\text{VII}_{\text{H-H}}$ indicates that each step, up to and including the formation of alkyl Breslow intermediate V_{P} must be reversible.⁸ This is not unexpected as the rate limiting step in this reaction is 3.6 kcal/mol lower than for the irreversible homo-benzoin of alkyl aldehydes.

Aryl–Alkyl Cross-Benzoin. Formation of the opposite cross-benzoin product is severely limited under reaction conditions. Following deprotonation of the triazolium salt as above, attack on benzaldehyde and subsequent protonation result in the formation of the aryl adduct, IV_{B} (Figure 4). This species is substantially higher in energy than IV_{P} at 3.8 kcal/mol (a 5.7 kcal/mol increase). An examination of the Mulliken charges suggests that the alkyl adduct is better able to evenly distribute the charge density, possibly due to the orientation of the hydroxyl group (See Supporting Information).

As with the alkyl adduct, attempts to find a transition state leading to the formation of IV_{B} were unsuccessful. An equivalent experiment was performed to gauge the efficiency of this step (Scheme 7). As before, within the first minute adduct was visible. The ratio of adduct to aldehyde remained relatively constant over

Scheme 7. Aryl Adduct Formation

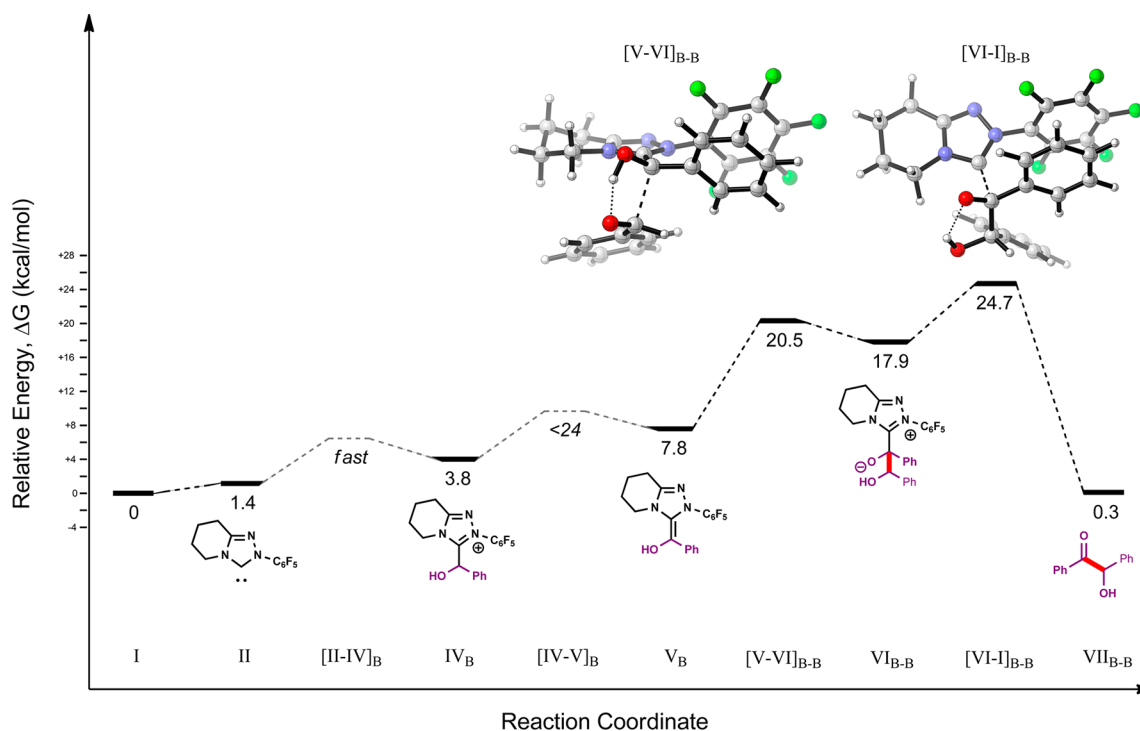
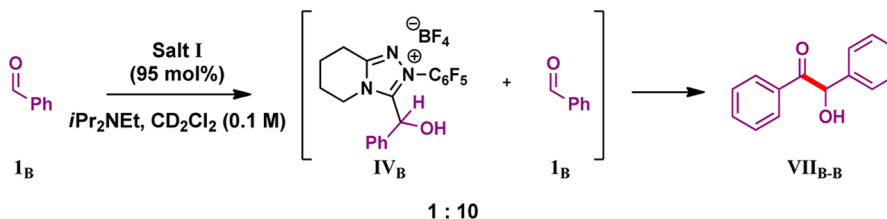


Figure 5. Aryl-aryl homo-benzoin reaction coordinate.

time despite steady consumption of both species to form homo-benzoin product. The 1:10 adduct-to-aldehyde mixture corresponds to an energy difference of ~ 1.4 kcal/mol between the two species. This may suggest that the energy of IV_P is also overestimated, though not necessarily.

The transition state leading to the formation of the aryl Breslow intermediate (V_B) remained as elusive as that for V_P . Previous work has shown the homo-benzoin reaction of benzaldehyde to be second order in aldehyde. During the cross-benzoin reaction a detectable amount of the homo-aryl product is observed, while typically no aryl-alkyl cross-benzoin product is seen. Given the similarity between the calculated energies of these pathways' rate-limiting steps (*vide infra*), it is unlikely to be a competitively rate-limiting step; the energy of this barrier is low relative to those of either of the later transition states, meaning formation of the Breslow intermediate cannot be rate-limiting.

As with the alkyl Breslow intermediate, V_B can adopt either an *E* or *Z* geometry. The *Z* isomer is slightly more stable than the *E* at 7.6 and 7.8 kcal/mol, respectively. Although the *Z* isomer possesses a path with a comparable rate-limiting barrier to that shown in Figure 4 (See Supporting Information), consideration of the *E* isomer provides better comparison to the reported path for the homo-benzoin reaction of benzaldehyde below.

Carbon-carbon bond formation is again the rate-limiting step with a barrier of 24.2 kcal/mol. A 2.7 kcal/mol preference for

attack on the *re* face of propionaldehyde results from an unfavorable steric interaction between the alkyl chain and phenyl ring in an attack on the *si* face. The resulting intermediate (VI_{B-P}) is slightly stabilized at 16.7 kcal/mol before ejection of the product occurs with a comparatively small barrier of 22.1 kcal/mol. This product is 2.0 kcal/mol more stable than the starting materials.

Aryl-Aryl Dimerization. The homo-benzoin reaction of aryl aldehydes presents a variety of deviations from the previous cases. The energy profile for this transformation is depicted in Figure 5. Formation of aryl Breslow intermediate V_B proceeds as above. The *E* isomer, slightly more energetic than the *Z*, is able to attack the *re* face of benzaldehyde with an activation energy of 20.1 kcal/mol. This transition state benefits from the same π -stacking/ π -cation interaction as in the case of the favored alkyl-aryl cross-benzoin above (Figure 3), and is 3.8 kcal/mol lower than any of its diastereomeric equivalents.

intermediate VI_{B-B} undergoes a rotation about the newly formed carbon-carbon bond and stabilizes at 17.9 kcal/mol. This rotation remains during the ejection of the homo-benzoin product ($[VI-I]_{B-B}$) at 24.7 kcal/mol. The rotation breaking the π -stacking/ π -cation interaction and change in rate-limiting steps from previous reactions were surprising; therefore, a variety of alternate conformations were examined (Figure 6). In $[VI-I]_{B-B(2)}$ the rotation has not occurred, maintaining the

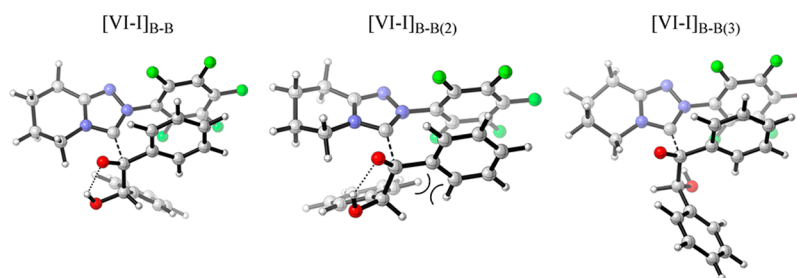
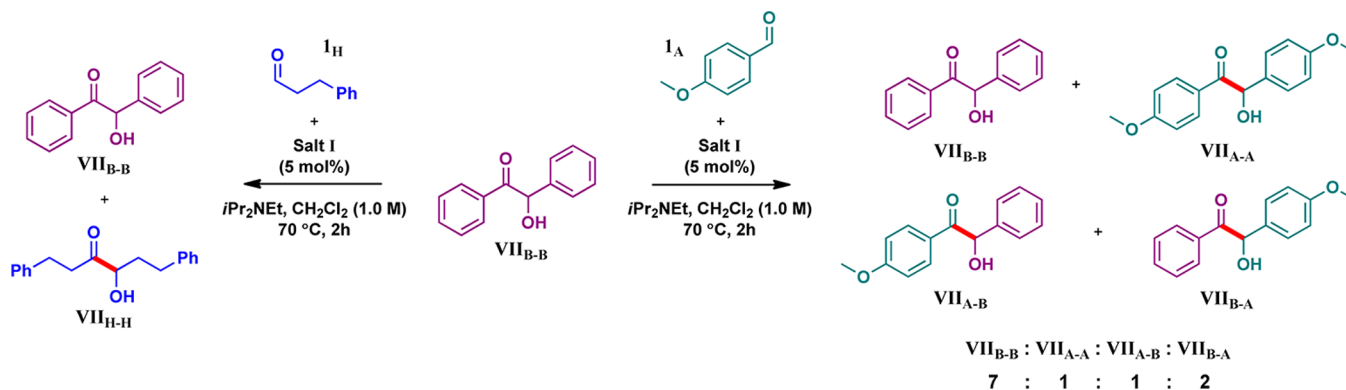


Figure 6. Aryl–aryl homo-benzoin ejection transition states.

Scheme 8. Homo-Aryl Crossover Experiment



π -stacking/ π -cation interaction. However, in this orientation the ortho protons of the two phenyl rings are relatively close (2.03 Å), resulting in a significant increase in energy; this transition state is 2.8 kcal/mol higher than $[\text{VI-I}]_{\text{B-B}}$. This interaction is only developing in the carbon–carbon bond formation step, suggesting that bond rotation likely occurs near the end of this transition ($[\text{V-VI}]_{\text{B-B}}$) to accommodate the growing strain. With a more extreme rotation, $[\text{VI-I}]_{\text{B-B(3)}}$ represents a non-hydrogen-bonded ejection. The loss of the hydrogen bonding is mitigated by π -stacking between all three aryl rings. Surprisingly, this transition state is 0.2 kcal/mol more stable than $[\text{V-VI}]_{\text{B-B}}$. As this rotation seems unlikely and the stabilization is within the error of the calculation, this ejection is discounted in favor of the traditional hydrogen-bonded one ($[\text{V-VI}]_{\text{B-B}}$).

The product is slightly higher in energy than the starting materials at +0.3 kcal/mol. Since the homo-benzoin reaction of benzaldehyde is known to proceed well under these conditions, this value must be an overestimate.³²

An intriguing pair of crossover experiments (Scheme 8) highlights the contrasting behavior of homo-aryl benzoin products in the presence of alkyl versus aryl aldehydes.

On the basis of the experiment with anisaldehyde, as well as the observation of a swift homo-benzoin reaction in the absence of alkyl aldehydes, formation of homo-aryl benzoin products is reversible. The barrier of 24.7 kcal/mol is not consistent with these factors; it must be slightly inflated. Observing the cross-benzoin reaction by ^1H NMR shows no initial buildup of $\text{VII}_{\text{B-B}}$, suggesting that its rate-limiting step has an activation barrier above 20.8 kcal/mol (i.e., higher than the kinetically favored pathway). The reaction is also reversible, necessitating a barrier lower than that of the irreversible homo-benzoin of alkyl aldehydes (24.4 kcal/mol). It is thus likely that the true rate-limiting barrier for this step is ~ 22 kcal/mol.

In the reaction with hydrocinnamaldehyde only the homo-alkyl product is formed and no retro-benzoin reaction for the

homo-aryl product is observed. This result is initially surprising, as it contradicts a similar experiment performed using the equivalent pyrrolidinone-derived catalyst.⁸ A possible justification for this can be made by considering the catalyst's strong preference for formation of the alkyl adduct. As the carbene is generated, it rapidly forms the more stable resting state IV_{H} , which then slowly attacks another 1 equiv of alkyl aldehyde, leading to the formation of $\text{VII}_{\text{H-H}}$. At no point during the reaction is there sufficient carbene in solution to catalyze the retro-benzoin reaction of the homo-aryl product. A similar argument could be made for the irreversibility of the homo-alkyl benzoin reaction; however, the crossover experiment with benzaldehyde (Scheme 5) should have sufficient carbene in solution to allow any potential retro-benzoin reaction to occur.

Electron-rich anisaldehyde has been shown to afford cross-benzoin product $\text{VII}_{\text{H-A}}$ in near-quantitative yield.¹⁷ Examination of the transition states for this reaction (see the Supporting Information) shows that the cross-benzoin pathway continues to have the lowest rate-limiting barrier, though it is slightly higher in energy (22.6 kcal/mol) than the cross-benzoin reaction involving benzaldehyde. Surprisingly, the improved yield can be attributed to a considerable increase in the energy of the rate-limiting ejection of the homo-aryl product; $[\text{VI-I}]_{\text{A-A}}$ has a barrier of 29.5 kcal/mol, representing a 4.8 kcal/mol increase over $[\text{VI-I}]_{\text{B-B}}$. This rise in energy can most likely be ascribed to the loss of a highly favorable rich–poor π -stacking interaction between the methoxylated and perfluorinated aromatic rings during the ejection of the product. An NCI analysis (see the Supporting Information) also shows a positive interaction between the methoxy and fluorine substituents, though the degree to which this affects the transition state is not obvious. Monitoring this reaction by ^1H NMR (see the Supporting Information) shows that the rate of product formation is roughly half that of the reaction between benzaldehyde and propanal and confirms that $\text{VII}_{\text{A-A}}$ is not observable at any point during the transformation.

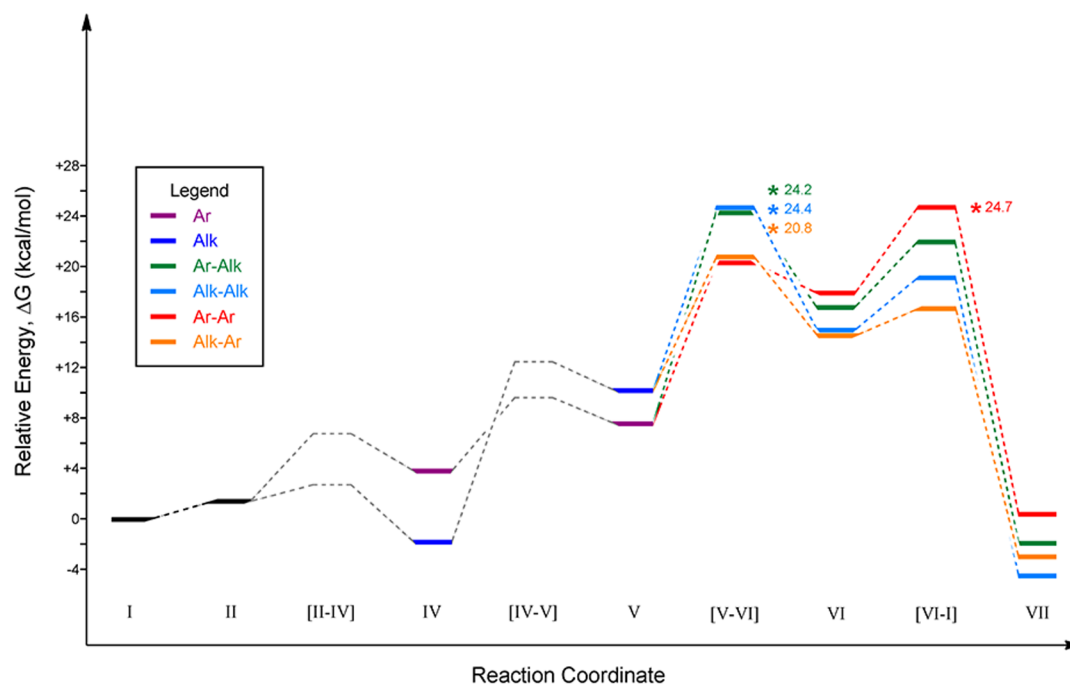


Figure 7. Overlaid benzoin reaction coordinates: piperidinone-based triazolium (I).

Pathway Comparison. An overlay of each reaction pathway (Figure 7) allows a summary of factors leading to chemoselectivity in the cross-benzoin reaction.

Deprotonation of the triazolium salt produces the active carbene catalyst, which either quickly attacks 1 equiv of alkyl aldehyde and collapses to a stable alkyl adduct or traverses a small barrier and forms a somewhat more energetic species with the aryl aldehyde. Both of these adducts must cross a potentially high, though not rate-limiting, barrier to form their respective Breslow intermediates. Attacks from either Breslow intermediate on aryl aldehydes are significantly favored through a stabilizing π -stacking/ π -cation interaction with the triazole ring. This step is rate-limiting for three potential paths: the homo-alkyl and both cross-benzoin reactions. Ejection of the benzoin product follows. For the homo-benzoin reaction of aryl aldehydes this step is rate-limiting, as steric interactions between the phenyl rings increase the energy of this step.

Additionally, the experimental results can be summarized by describing the reversible steps in the system (Scheme 9). Formation of all species up to and including the Breslow intermediates is completely reversible. In the formation of the homo-alkyl benzoin product either (or both) the carbon–carbon bond formation or ejection step is irreversible. On the basis of the calculated barriers for this path, it is more likely to be the carbon–carbon bond formation step. Both the formation of the alkyl–aryl cross-benzoin product and the homo-aryl benzoin product are reversible. The aryl–alkyl cross-benzoin reaction could not be probed to determine its reversibility. With a rate-limiting barrier on par with the homo-alkyl benzoin pathway, it is likely to be formed irreversibly, again with a probable irreversible carbon–carbon bond formation.

Pyrrolidinone-Based Triazolium. On the basis of the above calculations and experiments, the origin of chemoselectivity in the piperidinone-based triazolium catalyst is clear and kinetically derived. However, the dramatic improvement of this catalyst over the pyrrolidinone-derived equivalent remains surprising; no species in the cycle displays an obvious interaction

with the catalyst backbone that could explain this difference. In order to reconcile this, the same reaction coordinates were explored for the pyrrolidinone-based triazolium catalyst. An overlay of the minimum energy paths for these transformations is depicted in Figure 8, showing a familiar motif.

The paths for each of the benzoin reactions follow near-identical reaction coordinates for the pyrrolidinone- and piperidinone-derived catalysts. The major difference is that the transition states for the last two steps in this case are significantly lower than those for the piperidinone-based system. This suggests that the pyrrolidinone-based catalyst should display similar chemoselectivity under kinetically controlled conditions. At room temperature this reaction exhibits only a slight preference for the alkyl–aryl cross-benzoin product. Lowering the temperature of the system provides access to kinetically controlled conditions. However, a dramatic decrease in reactivity is also observed, and no reaction at all occurs at 0 °C. Monitoring the UV absorbance of a solution of in situ generated carbene over a range of temperatures (see the Supporting Information) suggests that carbene solubility is strongly temperature dependent; although kinetically controlled chemoselectivity may improve substantially at lower temperatures, there is insufficient solvated catalyst at these temperatures for an efficient reaction.

Under the optimal conditions for the piperidinone-derived catalyst, the pyrrolidinone-based catalyst displays a similar distribution of products (Scheme 10). This result is initially surprising. However, it can be rationalized by considering a thermodynamic equilibrium.

A 1:1 mix of the two aldehydes can, in a simplistic sense, result in three outcomes. These can be most easily understood by thinking of a set of four molecules: two molecules of an alkyl aldehyde and two of an aryl aldehyde. These can then form a set of the two homo-benzoin products (−4.3 kcal/mol), a pair of the aryl–alkyl cross-products (−4.0 kcal/mol), or a pair of the alkyl–aryl cross-products (−5.9 kcal/mol). Thus, in a 1:1 mixture of aryl and alkyl aldehydes the thermodynamically favored products are also the kinetically favored ones; the pyrrolidinone-based

Scheme 9. Reaction Path Summary

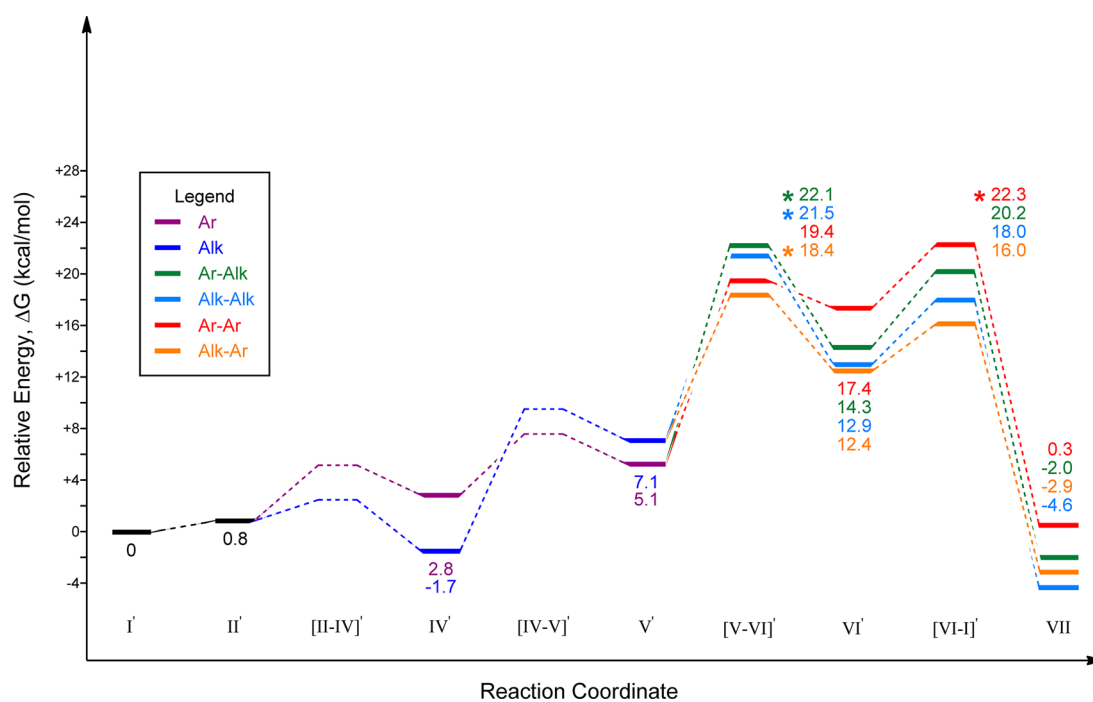
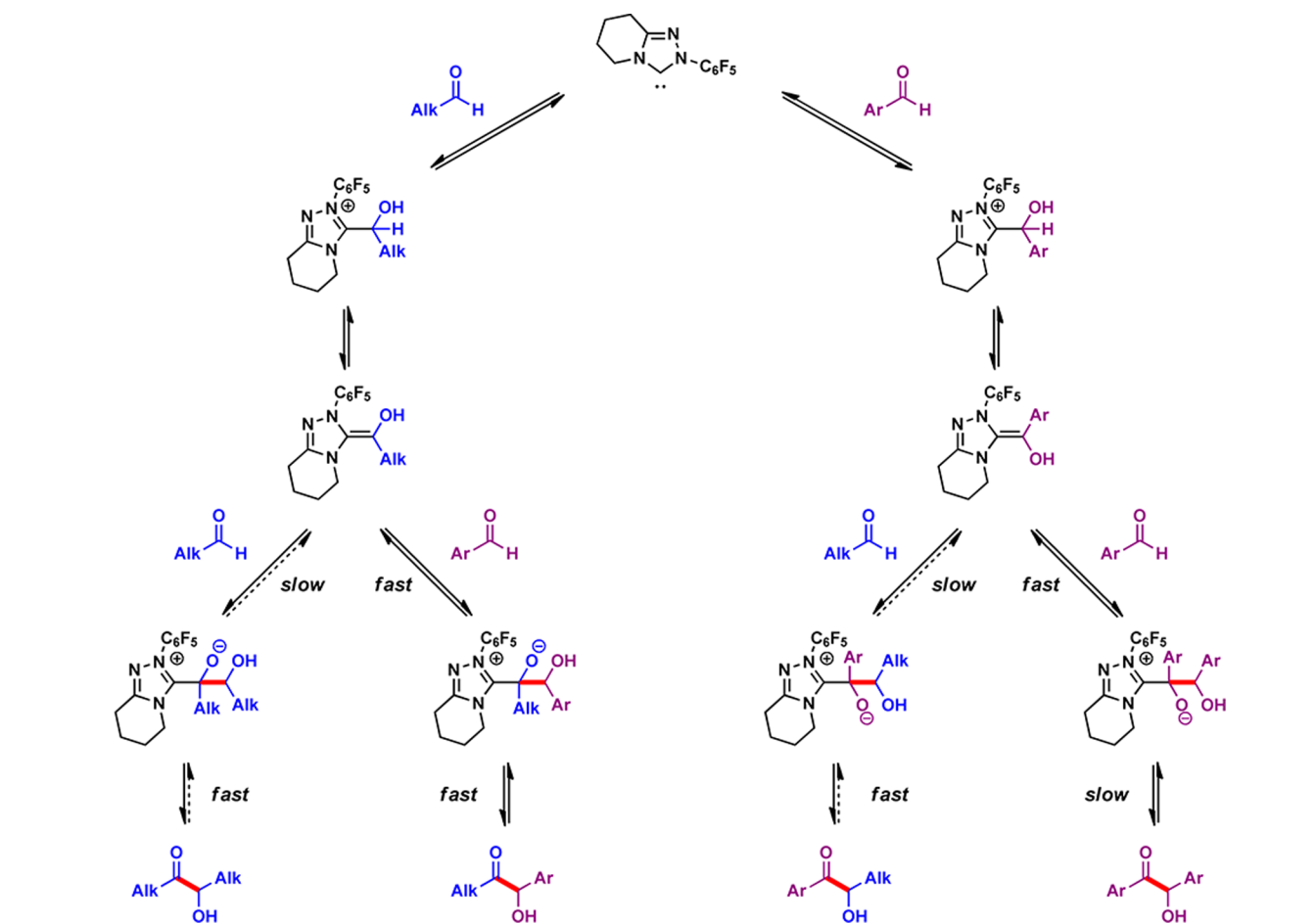


Figure 8. Overlaid benzoin reaction coordinates: pyrrolidinone-based triazolium (I').

triazolium is able to achieve a chemoselective cross-benzoin reaction through thermodynamic control. A crossover experiment confirms that even the previously irreversible formation of

the homo-alkyl product is now reversible, allowing equilibration to achieve chemoselectivity. This may be beneficial in some instances; however, it is likely not applicable to potential

Scheme 10. Chemoselective Cross-Benzoin Catalyzed by a Pyrrolidinone-Based NHC

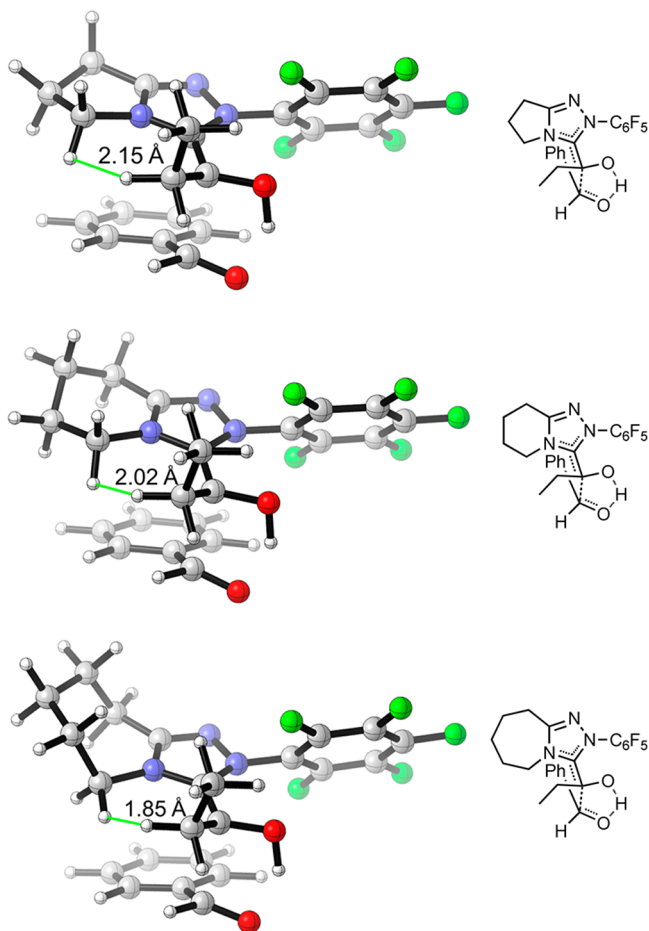
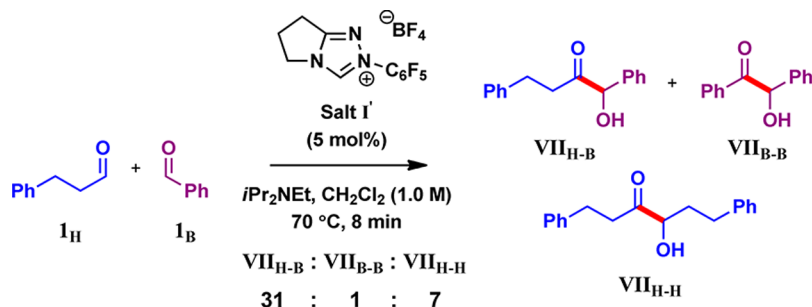


Figure 9. Increased steric interactions with increased catalyst backbone size.

enantioselective cross-benzoin reactions (which must rely on kinetically controlled conditions).

Effect of the Fused Ring. Complementary to the pyrrolidinone- and piperidinone-based triazoliums, a caprolactam-based catalyst (**I''**) was previously shown to catalyze the cross-benzoin reaction.¹⁷ Under suboptimal conditions this catalyst was found to have selectivity inferior to that of the piperidinone-derived system (**I**). However, repetition of this experiment suggests that this result is highly variable; disparate conversions and chemoselectivities in several attempts suggest that the reaction is significantly affected by trace moisture/oxygen, exacerbated by extended reaction times. To more accurately compare the three catalysts, ¹H NMR experiments were performed to monitor the reactions under conditions similar to those previously shown as optimal (see the Supporting

Information). Under these conditions a noticeable improvement in chemoselectivity is observed. These reactions show that each additional methylene group in the catalyst backbone decreases the rate of reaction by a factor of 5.

The transition state for the rate-limiting carbon–carbon bond formation of the cross-benzoin reaction catalyzed by the caprolactam-based triazolium (**[VI-I]''_{p-B}**) was modeled and found to have a barrier of 23.5 kcal/mol. The relative increase in this barrier for the piperidinone-based catalyst over the pyrrolidinone-based equivalent (+2.4 kcal/mol) is comparable to the corresponding increase for the piperidinone-based triazolium over the pyrrolidinone-derived species (+2.7 kcal/mol); each additional CH₂ unit in the catalyst backbone increases the barrier for this step by roughly 2.5 kcal/mol. This is consistent with the commensurate decrease in the rates of these reactions.

Examination of the transition states for these transformations (Figure 9) suggests that the proximal methylene protons of the catalyst backbone become increasingly close to those from the parent aldehyde chain. This steric interaction seems the most likely source for the proportional increases in energy between the transition states.

CONCLUSION

The origin of chemoselectivity in the triazolium-catalyzed cross-benzoin reaction has been explored. With the piperidinone-derived triazolium (**I**) catalyst, the chemoselectivity is determined kinetically. This is supported by computational and ¹H NMR studies, as well as a series of crossover experiments. The common pyrrolidinone-derived catalyst (**I'**) was found to display a strikingly similar energy profile for this reaction, despite experimental data showing that it is less chemoselective. Chemoselectivity could not be improved through kinetic control with this catalyst; however, equilibrating conditions show substantial preference for the same cross-benzoin product kinetically favored by the piperidinone-derived catalyst. A comparison of the rates and transition states of the reaction as catalyzed by the pyrrolidinone-, piperidinone-, and caprolactam-derived catalysts (**I'**, **I**, and **I''**, respectively) suggests that steric interactions play a significant role in obtaining chemoselectivity; too little leads to a thermodynamic mixture, and too much leads to a slow reaction susceptible to side reactions and degradation. Given the potential of cross-benzoin reactions in the construction of strategic C–C bonds, we hope this work will constitute a valuable resource in synthetic planning by providing a degree of understanding and predictability for this reaction.³³

EXPERIMENTAL SECTION

General Information. Nuclear magnetic resonance (NMR) spectra were recorded on an FT-NMR spectrometer with CD₂Cl₂ as solvent at 500 MHz for ¹H and 125 MHz for ¹³C. The residual solvent protons

(¹H) or the solvent carbons (¹³C) were used as internal standards for chemical shifts. High-resolution mass spectra (HRMS) were obtained on a double-focusing high-resolution spectrometer. Aliphatic aldehydes were distilled prior to use, and liquid aromatic aldehydes were distilled immediately before use. All reactions were carried out under an inert atmosphere of argon. Anhydrous solvents were stored under argon over 3 Å molecular sieves for at least 48 h. The moisture content was analyzed and at no time exceeded 15 ppm prior to use.

Procedure for Determination of Order of the Cross-Benzoin Reaction in Benzaldehyde. The triazolium salt I (9 mg, 0.025 mmol (0.05 equiv)) and dimethyl terephthalate (10 mg, 0.0083 mmol (internal standard)) were placed in an NMR tube under an argon atmosphere. Hydrocinnamaldehyde (66 μL, 0.5 mmol (1 equiv)) and toluene (0.50 mL, 1.0 M) were added. Benzaldehyde was varied in each experiment as outlined: 25 μL, 0.25 mmol (0.5 equiv); 50 μL, 0.5 mmol (1.0 equiv, run twice); 63 μL, 0.625 mmol (1.25 equiv); 75 μL, 0.75 mmol (1.5 equiv); 100 μL, 1.0 mmol (2.0 equiv); 125 μL, 1.25 mmol (2.5 equiv); 150 μL, 1.5 mmol (3.0 equiv). The tube was capped and sealed with Parafilm, shaken gently to dissolve all solids, and preheated in the spectrometer to 60 °C, and a spectrum was collected. As quickly as possible the sample cap was partially removed, premeasured (*i*-Pr)₂NEt base was added (87 μL, 0.5 mmol (1 equiv)), and the cap was resealed with Parafilm. The tube was inverted once for mixing and reinserted into the probe. A timer was started at the moment of base injection. Spectra were collected at marked intervals until ~80% consumption of hydrocinnamaldehyde (by internal standard). Plots of the yield of cross-benzoin product (by internal standard) versus time were fitted with second-order polynomials. The initial rates were determined by calculating the slope of the tangent at *t* = 0 s. A plot of the natural logarithms of these initial rates versus the natural logarithms of the concentrations shows that the reaction is, within error, first order in benzaldehyde. All spectra are consistent with those previously reported.

Procedure for Alkyl Adduct Formation and Reversibility (IV_H and IV_O). The triazolium salt I (18 mg, 0.0475 mmol (0.95 equiv)) and dimethyl terephthalate (10 mg, 0.0083 mmol (internal standard)) were placed in an NMR tube under an argon atmosphere. Hydrocinnamaldehyde (7 μL, 0.05 mmol (1 equiv)) and CD₂Cl₂ (0.50 mL, 0.1 M) were added. The tube was capped and sealed with Parafilm and shaken gently to dissolve all solids, and a spectrum was collected. As quickly as possible the sample cap was partially removed, premeasured (*i*-Pr)₂NEt base was added (9 μL, 0.05 mmol (1 equiv)), and the cap was resealed with Parafilm. The tube was inverted once for mixing and reinserted into the probe. A timer was started at the moment of base injection. Spectra were collected at marked intervals until no further changes were observed. After 197 s octanal (8 μL, 0.05 mmol (1 equiv)) was added in a similar fashion and additional spectra were collected. Additional experiments as above, but in the absence of octanal, were performed to confirm adduct stability. Characterization of the hydrocinnamaldehyde adduct was carried out using one such experiment. Attempts to isolate the adduct resulted in decomposition. ¹H NMR (500 MHz, CD₂Cl₂): δ 7.34–7.20 (m, 5H), 5.13 (s br, 1H), 4.38 (s br, 1H), 4.25 (s br, 1H), 3.00–2.92 (m, 2H), 2.82–2.79 (m, 2H), 2.26 (s br, 1H), 1.93–1.87 (m, 1H), additional signals obscured below 1.6. HRMS (ESI⁺): *m/z* calculated for C₂₁H₁₉N₃OF₅⁺ [M]⁺ 424.1443, found 424.1438.

Procedure for Aryl Adduct Formation (IV_B). The triazolium salt I (18 mg, 0.0475 mmol (0.95 equiv)) and dimethyl terephthalate (10 mg, 0.0083 mmol (internal standard)) were placed in an NMR tube under an argon atmosphere. Benzaldehyde (5 μL, 0.05 mmol (1 equiv)) and CD₂Cl₂ (0.50 mL, 0.1 M) were added. The tube was capped and sealed with Parafilm and shaken gently to dissolve all solids, and a spectrum was collected. As quickly as possible the sample cap was partially removed, premeasured (*i*-Pr)₂NEt base was added (9 μL, 0.05 mmol (1 equiv)), and the cap was resealed with Parafilm. The tube was inverted once for mixing and reinserted into the probe. A timer was started at the moment of base injection. Spectra were collected at marked intervals. Given the transient nature of the adduct, characterization could not be performed beyond in situ ¹H NMR. The characteristic peak

at 6.57 ppm is consistent with the values reported in the literature for similar adducts.^{30a}

Procedure for Competitive Adduct Formation (IV_H vs IV_B). The triazolium salt I (18 mg, 0.0475 mmol (0.95 equiv)) and dimethyl terephthalate (10 mg, 0.0083 mmol (internal standard)) were placed in an NMR tube under an argon atmosphere. Benzaldehyde (5 μL, 0.05 mmol (1 equiv)), hydrocinnamaldehyde (7 μL, 0.05 mmol (1 equiv)), and CD₂Cl₂ (1.0 mL, 0.05 M) were added. The tube was capped and sealed with Parafilm and shaken gently to dissolve all solids, and a spectrum was collected. As quickly as possible the sample cap was partially removed, premeasured (*i*-Pr)₂NEt base was added (9 μL, 0.05 mmol (1 equiv)), and the cap was resealed with Parafilm. The tube was inverted once for mixing and reinserted into the probe. A timer was started at the moment of base injection. Spectra were collected at marked intervals. The in situ ¹H NMR spectra were consistent with the formation of the hydrocinnamaldehyde adduct.

Procedure for Alkyl–Alkyl (VII_{H,H}) Crossover with Octanal. The triazolium salt I (7 mg, 0.018 mmol (0.05 equiv)) was placed in a test tube with a Schlenk takeoff which was then fitted with a septum and placed under an inert atmosphere. 4-Hydroxy-1,6-diphenylhexan-3-one (97 mg, 0.36 mmol (1 equiv)), octanal (56 μL, 0.36 mmol (1 equiv)), and CH₂Cl₂ (0.36 mL, 1 M) were added. Finally (*i*-Pr)₂NEt base was added (63 μL, 0.36 mmol (1 equiv)) and the septum was then quickly exchanged for a cold finger. Once an inert atmosphere was re-established, the flask was sealed and heated to 70 °C for 2 h and then quenched by washing with 2 M HCl and dried over Na₂SO₄. Dimethyl terephthalate was added as an internal standard. All spectra are consistent with those previously reported.

Procedure for Alkyl–Alkyl (VII_{H,H}) Crossover with Benzaldehyde. The triazolium salt I (7 mg, 0.018 mmol (0.05 equiv)) was placed in a test tube with a Schlenk takeoff which was then fitted with a septum and placed under an inert atmosphere. 4-Hydroxy-1,6-diphenylhexan-3-one (101 mg, 0.375 mmol (0.75 equiv)), benzaldehyde (50 μL, 0.5 mmol (1 equiv)), and CH₂Cl₂ (0.50 mL, 1 M) were added. Finally (*i*-Pr)₂NEt base was added (87 μL, 0.36 mmol (1 equiv)) and the septum was then quickly exchanged for a cold finger. Once an inert atmosphere was re-established, the flask was sealed and heated to 70 °C for 2 h and then quenched by washing with 2 M HCl and dried over Na₂SO₄. Dimethyl terephthalate was added as an internal standard. All spectra are consistent with those previously reported.

Procedure for Alkyl–Aryl (VII_{H,B}) Crossover with *p*-Anisaldehyde. The triazolium salt I (5 mg, 0.0133 mmol (0.05 equiv)) was placed in a test tube with a Schlenk takeoff which was then fitted with a septum and placed under an inert atmosphere. 1-Hydroxy-1,4-diphenylbutan-2-one (63 mg, 0.27 mmol (1 equiv)), *p*-anisaldehyde (33 μL, 0.27 mmol (1 equiv)), and CH₂Cl₂ (0.27 mL, 1 M) were added. Finally (*i*-Pr)₂NEt base was added (63 μL, 0.36 mmol (1 equiv)) and the septum was then quickly exchanged for a cold finger. Once an inert atmosphere was re-established, the flask was sealed and heated to 70 °C for 2 h and then quenched by washing with 2 M HCl and dried over Na₂SO₄. Dimethyl terephthalate was added as an internal standard. Attempts to separate the mixture of aryl cross-benzoin products led to decomposition or resulted in no separation. All spectra are consistent with those previously reported.

Procedure for Aryl–Aryl (VII_{B,B}) Crossover with Hydrocinnamaldehyde. The triazolium salt I (9 mg, 0.025 mmol (0.05 equiv)) was placed in a test tube with a Schlenk takeoff which was then fitted with a septum and placed under an inert atmosphere. 2-Hydroxy-1,2-diphenylethanone (106 mg, 0.25 mmol (0.5 equiv)), hydrocinnamaldehyde (99 μL, 0.75 mmol (1.5 equiv)), and CH₂Cl₂ (0.5 mL, 1 M) were added. Finally (*i*-Pr)₂NEt base was added (87 μL, 0.5 mmol (1 equiv)) and the septum was then quickly exchanged for a cold finger. Once an inert atmosphere was re-established, the flask was sealed and heated to 70 °C for 2 h and then quenched by washing with 2 M HCl and dried over Na₂SO₄. Dimethyl terephthalate was added as an internal standard. All spectra are consistent with those previously reported.

Procedure for Aryl–Aryl (VII_{B,B}) Crossover with *p*-Anisaldehyde. The triazolium salt I (9 mg, 0.025 mmol (0.05 equiv)) was placed in a test tube with a Schlenk takeoff which was then fitted with a septum

and placed under an inert atmosphere. 2-Hydroxy-1,2-diphenylethanolone (106 mg, 0.5 mmol (1 equiv)), *p*-anisaldehyde (61 μ L, 0.5 mmol (1 equiv)), and CH_2Cl_2 (0.5 mL, 1 M) were added. Finally (*i*-Pr)₂NEt base was added (87 μ L, 0.5 mmol (1 equiv)) and the septum was then quickly exchanged for a cold finger. Once an inert atmosphere was re-established, the flask was sealed and heated to 70 °C for 2 h and then quenched by washing with 2 M HCl and dried over Na_2SO_4 . Dimethyl terephthalate was added as an internal standard. Attempts to separate the mixture of aryl cross-benzoin products led to decomposition or resulted in no separation. All spectra are consistent with those previously reported.

Procedure for High Temperature Cross-Benzoin Reaction Catalyzed by the Pyrrolidinone-Based Triazolium (I'). The triazolium salt I' (9 mg, 0.025 mmol (0.05 equiv)) was placed in a test tube with a Schlenk takeoff which was then fitted with a septum and placed under an inert atmosphere. Benzaldehyde (50 μ L, 0.5 mmol (1 equiv)), hydrocinnamaldehyde (99 μ L, 0.75 mmol (1.5 equiv)), and CH_2Cl_2 (0.5 mL, 1.0 M) were added. Finally (*i*-Pr)₂NEt base was added (87 μ L, 0.5 mmol (1 equiv)) and the septum was then quickly exchanged for a cold finger. Once an inert atmosphere was re-established, the flask was sealed and heated to 70 °C for 8 min and then quenched by washing with 2 M HCl and dried over Na_2SO_4 . Dimethyl terephthalate was added as an internal standard. All spectra are consistent with those previously reported.

Procedure for Room Temperature Cross-Benzoin Reaction Catalyzed by the Pyrrolidinone-Based Triazolium (I'). The triazolium salt I' (9 mg, 0.025 mmol (0.05 equiv)) was placed in a test tube with a Schlenk takeoff which was then fitted with a septum and placed under an inert atmosphere. Benzaldehyde (50 μ L, 0.5 mmol (1 equiv)), hydrocinnamaldehyde (99 μ L, 0.75 mmol (1.5 equiv)), and CH_2Cl_2 (0.5 mL, 1.0 M) were added. Finally (*i*-Pr)₂NEt base was added (87 μ L, 0.5 mmol (1 equiv)) and the septum was then quickly exchanged for a cold finger. Once an inert atmosphere was re-established, the flask was sealed and heated to 70 °C for 8 min and then quenched by washing with 2 M HCl and dried over Na_2SO_4 . Dimethyl terephthalate was added as an internal standard. All spectra are consistent with those previously reported.

Procedure for Monitoring Solubility of the Pyrrolidinone-Based Carbene (II') as a Function of Temperature. The triazolium salt I' (0.6 mg, 0.0017 mmol (1 equiv)) was added to a quartz cuvette which was then sealed and placed under an inert atmosphere. CH_2Cl_2 (1.5 mL, 0.0011 M) was added. The cuvette was chilled to -5 °C, and (*i*-Pr)₂NEt base was added (6 μ L, 0.034 mmol (20 equiv)). The vessel was quickly shaken and reinserted in the spectrometer. The temperature was increased at a rate of 0.25 °C/min. Measurements of the absorbance at the 320 nm wavelength (previously determined maximum value) were recorded at each 0.5 °C increment.

Procedure for the Comparison of Reaction Rates. The triazolium salt (I, I', or I'') (0.025 mmol (0.05 equiv)) and dimethyl terephthalate (10 mg, 0.0083 mmol (internal standard)) were placed in an NMR tube under an argon atmosphere. Hydrocinnamaldehyde (66 μ L, 0.5 mmol (1 equiv)), benzaldehyde (50 μ L, 0.5 mmol (1 equiv)), and deuterated dichloromethane (0.50 mL, 1.0 mmol) were added. An additional reaction was performed using salt I with *p*-anisaldehyde (61 μ L, 0.5 mmol (1 equiv)) in place of benzaldehyde. The tube was capped and sealed with Parafilm, shaken gently to dissolve all solids, and preheated in the spectrometer to 35 °C, and a spectrum was collected. As quickly as possible the sample cap was partially removed, premeasured (*i*-Pr)₂NEt base was added (87 μ L, 0.5 mmol (1 equiv)), and the cap was resealed with Parafilm. The tube was inverted once for mixing and reinserted into the probe. A timer was started at the moment of base injection. Spectra were collected at marked intervals using a preprogrammed pulse sequence. The integration value for both aldehydes was plotted versus time. The slope of the lines connecting the first few (9–29) data points for both aldehydes was determined. Note that for the anisaldehyde cross-benzoin reaction only the rate of anisaldehyde consumption was used, as significant homo-alkyl formation lead to a deviation from comparable consumption rates. These lines were normalized for direct comparison. All spectra are consistent with those previously reported.

■ ASSOCIATED CONTENT

■ Supporting Information

Figures and tables giving computational results, spectra, and graphical data. This material is available free of charge via the Internet at <http://pubs.acs.org>.

■ AUTHOR INFORMATION

Corresponding Authors

*E-mail for C.Y.L.: claudel.legault@usherbrooke.ca.

*E-mail for M.G.: michel.gravel@usask.ca.

Notes

The authors declare no competing financial interest.

■ ACKNOWLEDGMENTS

We thank the Government of Saskatchewan for an Innovation and Opportunity Scholarship (to S.M.L.), the Natural Sciences and Engineering Research Council of Canada, the Canada Foundation for Innovation, Université de Sherbrooke, and the University of Saskatchewan for financial support. This research was enabled in part by support provided by WestGrid (www.westgrid.ca), Compute Canada Calcul Canada (www.computeCanada.ca), and Calcul Québec (www.calculquebec.ca). We wish to also thank Drs. Ian J. Burgess and Ronald P. Steer for useful discussions, as well as Myron M. D. Wilde for help during the early stages of the project.

■ REFERENCES

- (1) (a) Wöhler, F. L. *J. Ann. Pharm.* **1832**, *3*, 249–282. For a possible contender, see: (b) Stange, C. *Rep. Pharm.* **1824**, *16*, 80–107.
- (2) Ukai, T.; Tanaka, R.; Dokawa, T. *J. Pharm. Soc. Jpn.* **1943**, *63*, 296–300.
- (3) Breslow, R. *J. Am. Chem. Soc.* **1958**, *80*, 3719–3726.
- (4) (a) Enders, D.; Niemeier, O.; Henseler, A. *Chem. Rev.* **2007**, *107*, 5606–5655. (b) Moore, J. L.; Rovis, T. *Asymmetric Organocatalysis* **2009**, *291*, 77–144. (c) Phillips, E. M.; Chan, A.; Scheidt, K. A. *Aldrichim. Acta* **2009**, *42*, 55–66. (d) Chiang, P.-C.; Bode, J. W. In *N-Heterocyclic Carbenes: From Laboratory Curiosities to Efficient Synthetic Tools*; Díez-González, S.; Royal Society of Chemistry: Cambridge, U.K., 2010; p 339. (e) Campbell, C. D.; Ling, K. B.; Smith, A. D. In *Carbene Catalysts*. Springer: Dordrecht, Germany, 2011; Vol. 32, p 263. (f) Grossmann, A.; Enders, D. *Angew. Chem., Int. Ed.* **2012**, *51*, 314–325. (g) Bugaut, X.; Glorius, F. *Chem. Soc. Rev.* **2012**, *41*, 3511–3522. (h) Thai, K. Sánchez-Larios, E.; Gravel, M. *N-Heterocyclic Carbenes in Organocatalysis*. In *Comprehensive Enantioselective Organocatalysis: Catalysts, Reactions, and Applications*; Dalko, P. I., Ed.; Wiley-VCH: Weinheim, Germany, 2013; pp 495–522. (i) O'Bryan, E. A.; Scheidt, K. A. *Acyloin Coupling Reactions*. In *Comprehensive Organic Synthesis II*, 2nd ed.; Marek, I., Knochel, P., Eds.; Elsevier: Amsterdam, 2014; Vol. 3, pp 621–655. (j) Bugaut, X. *Benzoin and Aza-benzoin*. In *Comprehensive Organic Synthesis II*; Marek, I., Knochel, P., Eds.; Elsevier: Amsterdam, 2014; Vol. 1, pp 424–470. (k) Hopkinson, M. N.; Richter, C.; Schedler, M.; Glorius, F. *Nature* **2014**, *510*, 485–496.
- (5) Lapworth, A. *J. Chem. Soc. Trans.* **1903**, *83*, 995–1005.
- (6) (a) Wittig, G.; Davis, P.; Koenig, G. *Chem. Ber. Recl.* **1951**, *84*, 627–632. (b) Seebach, D. *Angew. Chem., Int. Ed. Engl.* **1979**, *18*, 239–258.
- (7) For an excellent summary of early work on the homo-benzoin reaction, see ref 4a. For more recent enantioselective work, see: (a) Enders, D.; Kallfass, U. *Angew. Chem., Int. Ed.* **2002**, *41*, 1743–1745. (b) Ma, Y. J.; Wei, S. P.; Wu, J.; Yang, F.; Liu, B.; Lan, J. B.; Yang, S. Y.; You, J. S. *Adv. Synth. Catal.* **2008**, *350*, 2645–2651. (c) Enders, D.; Han, J. W. *Tetrahedron: Asymmetry* **2008**, *19*, 1367–1371. (d) Baragwanath, L.; Rose, C. A.; Zeitler, K.; Connon, S. J. *J. Org. Chem.* **2009**, *74*, 9214–9217. (e) Soeta, T.; Tabatake, Y.; Inomata, K.; Ukaji, Y. *Tetrahedron* **2012**, *68*, 894–899.
- (8) O'Toole, S. E.; Rose, C. A.; Gundala, S.; Zeitler, K.; Connon, S. J. *J. Org. Chem.* **2011**, *76*, 347–357.

- (9) (a) Hachisu, Y.; Bode, J. W.; Suzuki, K. *J. Am. Chem. Soc.* **2003**, *125*, 8432–8433. (b) Enders, D.; Niemeier, O.; Balensiefer, T. *Angew. Chem., Int. Ed.* **2006**, *45*, 1463–1467. (c) Enders, D.; Niemeier, O.; Raabe, G. *Synlett* **2006**, 2431–2434. (d) Takikawa, H.; Hachisu, Y.; Bode, J. W.; Suzuki, K. *Angew. Chem., Int. Ed.* **2006**, *45*, 3492–3494. (e) Li, Y.; Feng, Z.; You, S. L. *Chem. Commun.* **2008**, 2263–2265. (f) Ema, T.; Oue, Y.; Akihara, K.; Miyazaki, Y.; Sakai, T. *Org. Lett.* **2009**, *11*, 4866–4869. (g) Takada, A.; Hashimoto, Y.; Takikawa, H.; Hikita, K.; Suzuki, K. *Angew. Chem., Int. Ed.* **2011**, *50*, 2297–2301. (h) Izquierdo, J.; Hutson, G. E.; Cohen, D. T.; Scheidt, K. A. *Angew. Chem., Int. Ed.* **2012**, *51*, 11686–11698. (i) Mennen, S. M.; Miller, S. J. *J. Org. Chem.* **2007**, *72*, 5260–5269.
- (10) (a) Stetter, H.; Dambkes, G. *Synthesis* **1977**, 403–404. (b) Jin, M. Y.; Kim, S. M.; Mao, H.; Ryu, D. H.; Song, C. E.; Yang, J. W. *Org. Biomol. Chem.* **2014**, *12*, 1547–1550. (c) Jin, M. Y.; Kim, S. M.; Han, H.; Ryu, D. H.; Yang, J. W. *Org. Lett.* **2011**, *13*, 880–883.
- (11) (a) Piel, I.; Pawelczyk, M. D.; Hirano, K.; Frohlich, R.; Glorius, F. *Eur. J. Org. Chem.* **2011**, 5475–5484. (b) Rose, C. A.; Gundala, S.; Connon, S. J.; Zeitler, K. *Synthesis* **2011**, 190–198.
- (12) (a) Enders, D.; Henseler, A. *Adv. Synth. Catal.* **2009**, *351*, 1749–1752. (b) Enders, D.; Henseler, A.; Lowins, S. *Synthesis* **2009**, 4125–4128. (c) Enders, D.; Grossmann, A.; Fronert, J.; Raabe, G. *Chem. Commun.* **2010**, 46, 6282–6284.
- (13) (a) Rose, C. A.; Gundala, S.; Fagan, C. L.; Franz, J. F.; Connon, S. J.; Zeitler, K. *Chem. Sci.* **2012**, *3*, 735–740. (b) Thai, K.; Langdon, S. M.; Bilodeau, F.; Gravel, M. *Org. Lett.* **2013**, *15*, 2214–2217.
- (14) (a) Enders, D.; Niemeier, O. *Synlett* **2004**, 2111–2114. (b) Takikawa, H.; Suzuki, K. *Org. Lett.* **2007**, *9*, 2713–2716. (c) Kuhl, N.; Glorius, F. *Chem. Commun.* **2011**, *47*, 573–575.
- (15) Mathies, A. K.; Mattson, A. E.; Scheidt, K. A. *Synlett* **2009**, 377–383.
- (16) (a) Dunkelmann, P.; Kolter-Jung, D.; Nitsche, A.; Demir, A. S.; Siegert, P.; Lingen, B.; Baumann, M.; Pohl, M.; Muller, M. *J. Am. Chem. Soc.* **2002**, *124*, 12084–12085. (b) Muller, C. R.; Perez-Sanchez, M.; de Maria, P. D. *Org. Biomol. Chem.* **2013**, *11*, 2000–2004. (c) Demir, A. S.; Sesenoglu, O.; Dunkelmann, P.; Muller, M. *Org. Lett.* **2003**, *5*, 2047–2050. (d) Stillger, T.; Pohl, M.; Wandrey, C.; Liese, A. *Org. Process Res. Dev.* **2006**, *10*, 1172–1177. (e) Pohl, M.; Lingen, B.; Muller, M. *Chem. - Eur. J.* **2002**, *8*, 5288–5295. (f) Demir, A. S.; Sesenoglu, O.; Eren, E.; Hosrik, B.; Pohl, M.; Janzen, E.; Kolter, D.; Feldmann, R.; Dunkelmann, P.; Muller, M. *Adv. Synth. Catal.* **2002**, *344*, 96–103.
- (17) Langdon, S. M.; Wilde, M. M. D.; Thai, K.; Gravel, M. *J. Am. Chem. Soc.* **2014**, *136*, 7539–7542.
- (18) (a) Yamabe, S.; Yamazaki, S. *Org. Biomol. Chem.* **2009**, *7*, 951–961. (b) He, Y. Q.; Xue, Y. *J. Phys. Chem. A* **2010**, *114*, 9222–9230.
- (19) (a) Kuniyil, R.; Sunoj, R. B. *Org. Lett.* **2013**, *15*, 5040–5043. (b) Hawkes, K. J.; Yates, B. F. *Eur. J. Org. Chem.* **2008**, 5563–5570. (c) Domingo, L. R.; Zaragoza, R. J.; Saez, J. A.; Arno, M. *Molecules* **2012**, *17*, 1335–1353. (d) Ajitha, M. J.; Suresh, C. H. *Tetrahedron Lett.* **2013**, *54*, 7144–7146.
- (20) Dudding, T.; Houk, K. N. *Proc. Natl. Acad. Sci. U.S.A.* **2004**, *101*, 5770–5775.
- (21) He, Y.-Q.; Xue, Y. *J. Phys. Chem. A* **2011**, *115*, 1408–1417.
- (22) Holloczki, O.; Kelemen, Z.; Nyulaszi, L. *J. Org. Chem.* **2012**, *77*, 6014–6022.
- (23) Berkessel, A.; Elfert, S.; Etzenbach-Effers, K.; Teles, J. H. *Angew. Chem., Int. Ed.* **2010**, *49*, 7120–7124.
- (24) Frisch, M. J.; Trucks, G. W.; Schlegel, H. B.; Scuseria, G. E.; Robb, M. A.; Cheeseman, J. R.; Scalmani, G.; Barone, V.; Mennucci, B.; Petersson, G. A.; Nakatsuji, H.; Caricato, M.; Li, X.; Hratchian, H. P.; Izmaylov, A. F.; Bloino, J.; Zheng, G.; Sonnenberg, J. L.; Hada, M.; Ehara, M.; Toyota, K.; Fukuda, R.; Hasegawa, J.; Ishida, M.; Nakajima, T.; Honda, Y.; Kitao, O.; Nakai, H.; Vreven, T.; Montgomery, J. A., Jr.; Peralta, J. E.; Ogliaro, F.; Bearpark, M. J.; Heyd, J.; Brothers, E. N.; Kudin, K. N.; Staroverov, V. N.; Kobayashi, R.; Normand, J.; Raghavachari, K.; Rendell, A. P.; Burant, J. C.; Iyengar, S. S.; Tomasi, J.; Cossi, M.; Rega, N.; Millam, N. J.; Klene, M.; Knox, J. E.; Cross, J. B.; Bakken, V.; Adamo, C.; Jaramillo, J.; Gomperts, R.; Stratmann, R. E.; Yazyev, O.; Austin, A. J.; Cammi, R.; Pomelli, C.; Ochterski, J. W.; Martin, R. L.; Morokuma, K.; Zakrzewski, V. G.; Voth, G. A.; Salvador, P.; Dannenberg, J. J.; Dapprich, S.; Daniels, A. D.; Farkas, Ö.; Foresman, J. B.; Ortiz, J. V.; Cioslowski, J.; Fox, D. J. *Gaussian 09, Revision C.01*; Gaussian, Inc., Wallingford, CT, USA, 2009.
- (25) Zhao, Y.; Truhlar, D. G. *Theor. Chem. Acc.* **2008**, *120*, 215–241.
- (26) Scalmani, G.; Frisch, M. J. *J. Chem. Phys.* **2010**, *132*, 114110.
- (27) Marenich, A. V.; Cramer, C. J.; Truhlar, D. G. *J. Phys. Chem. B* **2009**, *113*, 6378–6396.
- (28) (a) Johnson, E. R.; Keinan, S.; Mori-Sanchez, P.; Contreras-Garcia, J.; Cohen, A. J.; Yang, W. T. *J. Am. Chem. Soc.* **2010**, *132*, 6498–6506. (b) Contreras-Garcia, J.; Johnson, E. R.; Keinan, S.; Chaudret, R.; Piquemal, J. P.; Beratan, D. N.; Yang, W. T. *J. Chem. Theory Comput.* **2011**, *7*, 625–632.
- (29) Legault, C. Y. *CYLView, 1.0b*; Université de Sherbrooke, Sherbrooke, Quebec, Canada, 2009; <http://www.cylview.org>.
- (30) (a) Collett, C. J.; Massey, R. S.; Maguire, O. R.; Batsanov, A. S.; O'Donoghue, A. C.; Smith, A. D. *Chem. Sci.* **2013**, *4*, 1514–1522. (b) Doleschall, G.; Tóth, G. *Tetrahedron* **1980**, *36*, 1649–1665. (c) Wendeborn, S.; Mondiere, R.; Keller, I.; Nussbaumer, H. *Synlett* **2012**, 541–544. Previous works have focused on the formation of aryl adducts (Smith) or observed only trace formation at catalytic loadings by mass spectrometry.
- (31) Breslow, R.; Kim, R. *Tetrahedron Lett.* **1994**, *35*, 699–702.
- (32) This reaction is known to proceed under a variety of conditions; the products must be more stable than the starting materials. A higher level of theory (CCSD(T)/LPNO-CEPA/1 extrapolation using the cc-PV(D/T)Z basis set) did not improve this discrepancy. Use of Grimme's D3 correction lowers this energy to -0.29 kcal/mol, though this value is likely still overestimated. (a) Grimme, S.; Antony, J.; Ehrlich, S.; Krieg, S. *J. Chem. Phys.* **2010**, *132*, 154104. (b) Goerigk, L.; Gimme, S. *Phys. Chem. Chem. Phys.* **2011**, *13*, 6670–6688.
- (33) As this paper was undergoing revisions, an article was published describing a computational study on this transformation. The conclusions of said manuscript, in our view, do not correspond with the experimental data described herein, nor that of our previous work (viz. the order of the reaction). Liu, T.; Han, S.; Han, L.; Wang, L.; Cui, X.; Du, C.; Bi, S. *Org. Biomol. Chem.* **2015**, DOI: 10.1039/C4OB02064B.